ELSEVIER

International Journal of Mass Spectrometry 197 (2000) 197–209

International Journal of Mass Spectrometry

Single photon and femtosecond multiphoton ionisation of the dipeptide valyl-valine

N.P. Lockyer*, J.C. Vickerman

Surface Analysis Research Centre, Department of Chemistry, UMIST, Manchester M60 1QD, UK

Received 16 September 1999; accepted 25 October 1999

Abstract

Femtosecond nonresonant multiphoton ionisation (fs-MPI) of the fragile biomolecule valyl-valine is compared with single photon ionisation (SPI) using time-of-flight mass spectrometry. Under conditions of comparable total ion yield the least amount of molecular ion dissociation is observed with 118 nm SPI (100 nJ cm^{-2}) followed by 266 nm fs-MPI (25 mJ cm^{-2}), then 400 nm, and 800 nm fs-MPI (230 mJ cm^{-2} and 1.3 J cm^{-2}, respectively). The laser intensity dependence of the ion signal observed at 266 nm and 400 nm is consistent with a simple nonresonant MPI mechanism whereas at 800 nm the results suggest a transition from the MPI regime toward a field ionisation mechanism such as tunneling or barrier suppression ionisation. (Int J Mass Spectrom 197 (2000) 197–209) © 2000 Elsevier Science B.V.

Keywords: Photoionisation; Photofragmentation; Femtosecond pulses; Vacuum ultraviolet

1. Introduction

The detection of trace quantities of important biochemicals using laser ionisation in conjunction with time-of-flight mass spectrometry is an area of considerable research activity. Typically analytes are desorbed into the gas phase by some prompt energy deposition mechanism, e.g. laser [1–3] or keV ion beam [4–6] desorption and ionised in the gas phase by application of a pulsed laser beam.

Resonance-enhanced multiphoton ionisation (REMPI) with nanosecond lasers is an established mass spectrometric technique that has enabled many organic molecules to be detected with extremely high sensitivity and minimal fragmentation [1–6]. This is achieved by resonantly pumping a specific intermediate electronic state in the target molecule thereby imparting a high degree of selectivity. This approach is successful provided the intermediate state lifetime is greater than the pulse width of the laser. If a chromophoric group is absent, depopulation of the intermediate state occurs on the subnanosecond timescale and nanosecond laser ionisation yields greatly reduced sensitivity and extensive fragmentation, often resulting in complete loss of molecular information. In some important biological systems such as polypeptides, extensive fragmentation is unavoidable even when resonantly excited at threshold laser powers due to fast ($>10^9$ s^{-1}) internal conversion and neutral dissociation mechanisms [7,8]. The fragmentation is more severe if rovibrational cooling of intermediate electronic levels, e.g. by supersonic jet entrainment is not used. Clearly, conventional nano-

* Corresponding author. E-mail: Nick.Lockyer@umist.ac.uk

PII S1387-3806(99)00249-3

second MPI mass spectrometry is unsuitable as a general, high efficiency method for detecting unknown biological species.

Studies with subpicosecond laser pulses show that in some instances neutral dissociation channels can be effectively bypassed using ultrashort high-intensity laser pulses [9–17]. Ionisation on a timescale shorter than that of intramolecular relaxation enhances molecular ion formation. However, the vast majority of published work concerning subpicosecond MPI of molecular species has involved chromophore-containing systems or simple di- or tri-atomics. It is of interest therefore to evaluate the effectiveness of fs-MPI for the more general case of polyatomic nonresonant photon excitation. This issue is addressed in the current study.

Single photon ionisation (SPI) in which intermediate molecular energy levels are not required also shows promise as a method of efficient ionisation for fragile systems [18–22]. With relatively low fluences of photons of sufficient energy to ionise a neutral molecule in a single step, photofragmentation resulting from multiple photon absorption can be effectively eliminated. Typically, some degree of fragmentation is observed in fragile systems because of the excess energy of the photoion following vacuum ultraviolet (VUV) photon excitation. SPI has the advantage over MPI in that chromophores are unnecessary and ionisation cross sections are relatively uniform from species to species.

In this article the femtosecond MPI and SPI mass spectrometric behaviour of a nonchromophore-containing system is described. The use of femtosecond pulses at 266, 400, and 800 nm and nanosecond 118 nm pulses for laser ionisation time-of-flight mass spectrometry is compared. We report in detail on the ionisation and fragmentation characteristics of the dipeptide valyl-valine that is representative of a fragile biomolecular system that has traditionally been unsuited to laser ionisation techniques. The structure of valyl-valine is shown in Scheme 1.

The photophysics of the laser ionisation event are also discussed. The mechanism of photoionisation at ultrahigh intensity is a subject of considerable interest from a fundamental and analytical standpoint. It has

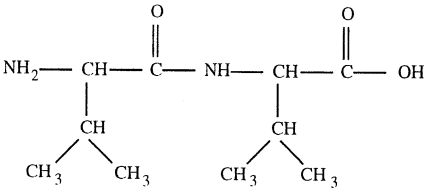

Scheme 1. Valyl-valine molecule.

been established that the mechanism of conventional MPI experiments ($<10^9$ W cm^{-2}) is governed by perturbation theory [23]. The advent of ultrahigh intensity laser pulses ($>10^{12}$ W cm^{-2}) offers the possibility of alternative ionisation mechanisms that require a semiquantum mechanical treatment. As the electric field strength associated with the laser approaches the binding energy of valance electrons the atomic or molecular potential surface becomes distorted. As the laser intensity increases so does the probability that valence electrons can tunnel through the coulombic barrier leading to tunnel ionisation (TI). The multiphoton and tunnel ionisation regimes can be quantitatively differentiated by the unitless Keldysh parameter γ [24]

$$\gamma = \left(\frac{E}{2\Phi}\right)^{1/2}$$

where E is the ionisation potential of the atom in eV and Φ is the ponderomotive potential (or *wiggle* energy) of the laser given by

$$\Phi(\text{eV}) = (9.33 \times 10^{-14}) I(\text{W cm}^{-2})\lambda^2(\mu\text{m})$$

The dominant ionisation regime is believed to be MPI where $\gamma > 5$ and TI where $\gamma < 0.5$ [25,26].

At a critical laser electric field strength the barrier to ionisation is lowered to such an extent that the electron can freely escape without tunneling. This is termed barrier suppression ionisation (BSI) [25,27] and occurs at a laser intensity threshold:

$$I_{\text{th}}(\text{W cm}^{-2}) = 4.00 \times 10^9\, E^4\,(\text{eV})/Z^2$$

where Z is the ionic charge. The TI and BSI models were developed for atomic ionisation but have been successfully incorporated into discussions on high

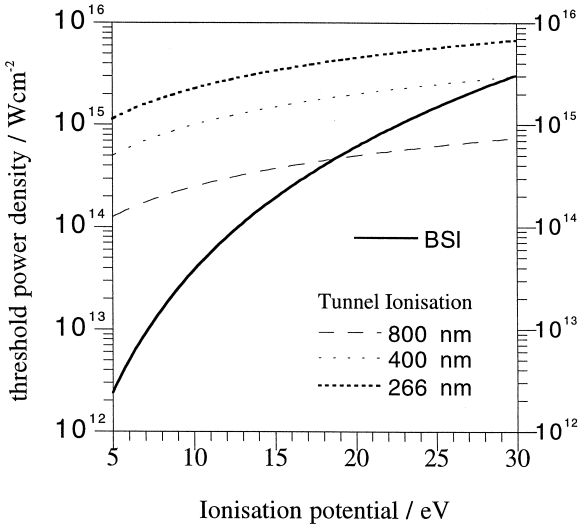

Fig. 1. Threshold laser intensities for barrier suppression ionisation and tunnel ionisation using 266, 400, and 800 nm photons.

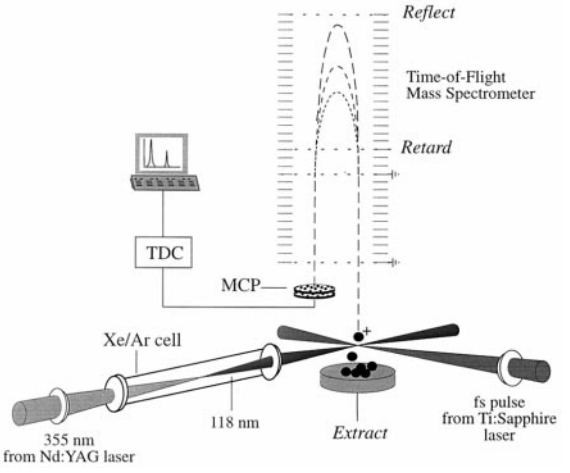

Fig. 2. Diagram of laser time-of-flight mass spectrometer.

intensity molecular ionisation mechanisms [28–32], therefore we have invoked these models in our discussion of results to aid mechanistic interpretation of the ionisation processes. Fig. 1 illustrates the threshold laser intensity as a function of ionisation potential required for barrier suppression ionisation and for tunnel ionisation ($\gamma = 0.5$) at the laser wavelengths used in this work.

2. Experimental

Experiments were performed in a dual-stage reflectron time-of-flight mass spectrometer (Fig. 2) with a base pressure of 5×10^{-9} mb. Valyl-valine (>99% purity, Sigma Chemical, Poole, UK) was deposited on a copper stub from methanolic solution and the solvent evaporated at room temperature prior to analysis. Analyte molecules were thermally desorbed (150 °C) in the source region of the mass spectrometer resulting in a measured pressure of 5×10^{-8} mb.

For the fs-MPI work the fundamental (800 nm) and the second (400 nm) and third (266 nm) harmonics of a 1 kHz Ti:sapphire laser (Clark-MXR) were used. The Ti:sapphire laser produces pulse widths (full width at half maximum) of 130 fs (800 nm), 230 fs (400 nm), and 250 fs (266 nm). The femtosecond laser system is described in detail elsewhere [10,11].

For SPI studies 118 nm radiation is generated by frequency tripling the third harmonic (355 nm) of a 5 ns, 10 Hz Nd:YAG laser (Spectra-Physics DCR-11). This is achieved in a gas cell attached to the laser entry window of the spectrometer containing a mixture of Xe and Ar gas under phase-matched conditions [33,34]. The design and operation of the frequency-tripling cell are described elsewhere [35].

The laser beams are focused to a diameter of several hundred microns by a MgF_2 lens mounted on an x, y, z manipulator and pass as close to the sample surface as possible without initiating laser desorption in order to maximise the overlap with the desorbed neutrals. The effective ionisation volume is controlled by translating the focusing lens along the axis of the laser beam. For fs-MPI experiments the laser power is controlled by altering the beam polarisation at the entrance to the compressor stage of the Ti:sapphire laser.

The sample surface is biased at a potential of 2.50 kV, establishing an electric field that extracts photoions into the mass spectrometer. After passing through a field-free drift region ions are energy refocused in a dual-stage reflectron and deflected onto a microchannel plate (MCP) detector. Ion arrival events are recorded by a time-to-digital converter

(TDC) and displayed on a PC. A diagram of the experimental method is shown in Fig. 2.

3. Results and discussion

The mass spectral ionisation behaviour of valyl-valine is presented in order to determine the optimum conditions for maximising the information content of the analysis. A detailed study of fs-MPI is compared to the results obtained with SPI. The efficiency of the ionisation and the degree of fragmentation induced are two aspects of the photoionisation process that are of particular importance to high-sensitivity mass spectrometric detection of complex molecules.

3.1. Threshold ionisation

Slow thermal desorption is a gentle process imparting relatively little fragmentation compared to prompt desorption mechanisms. As such it allows an investigation of the fragmentation associated with the ionisation event with minimal interference from the desorption mechanism. The SPI and fs-MPI mass spectra of valyl-valine obtained at threshold laser intensity are shown in Fig. 3. The normalised intensity values of the diagnostic fragments are given in Table 1. The observation of diagnostic fragment ions can aid spectral interpretation of complex biomolecules. At threshold laser power density (2×10^{10} W cm^{-2}) 266 nm fs-MPI yields the greatest fraction of nondissociated molecular ion and high-mass fragments [Fig. 3(b)]. Under these conditions the majority of photoions are produced by a two-photon absorption imparting a total of 9.32 eV of energy into the neutral molecule. This is less than the 118 nm photon energy (10.5 eV), which might explain why the SPI results in a much more intense immonium ion, in addition to the intact molecular ion [Fig. 3(a)]. Note that the intensity scale is expanded in Fig. 3(a) to allow observation of the low relative intensity peaks. Molecular ion intensities of a few percent have previously been observed in SPI of laser-desorbed dipeptides [20]. These data were acquired with the same laser beam diameter and at the same neutral density of analyte so it can be assumed that the number of neutral molecules probed is approximately equal in each case. The SPI data was summed over 4000 laser shots and the fs-MPI data summed over 50 000 laser shots. If the photoion signal intensity is normalised to the number of laser shots the molecular ion signal (*m/z* 216) and the immonium ion signal (*m/z* 72) are approximately one and two orders of magnitude, respectively, larger in the SPI spectra.

The 400 nm (2×10^{11} W cm^{-2}) and 800 nm (2×10^{12} W cm^{-2}) fs-MPI mass spectra show a similar degree of fragmentation to each other, with the complete loss of the molecular ion [Fig. 3(c), (d)]. The threshold laser intensities for observable photoion signal with 400 nm and 800 nm photons are, respectively, one and two orders of magnitude higher than at 266 nm because of the increase in the photon order of the ionisation mechanism at the longer wavelengths.

3.2. Photofragmentation mechanism

An understanding of the influence of the laser intensity on the branching ratios in the mass spectra is of vital importance in establishing optimum conditions for molecular analysis. The intensity dependence of the yield of fragment ions was measured for fs-MPI. In order to initiate fragmentation additional photon absorption may be required by the parent species. For fragment ions, lowest-order perturbation theory (LOPT) predicts that the gradient of a log–log plot of signal intensity against laser intensity describes the number of photons required for the formation of that ion [36,37]. Complications arise where fragment ions have more than one formation mechanism involving different photon numbers or where fragments themselves further dissociate into smaller products.

At 266 nm (Fig. 4), the individual fragment ions display a range of power dependencies from 1.2 to 2.3 (Table 2). All fragments except *m/z* 56 (val-NH_2COOH) display a decrease in gradient in the region of 10^{11} W cm^{-2} that is consistent with the preferential formation of lower mass fragments by

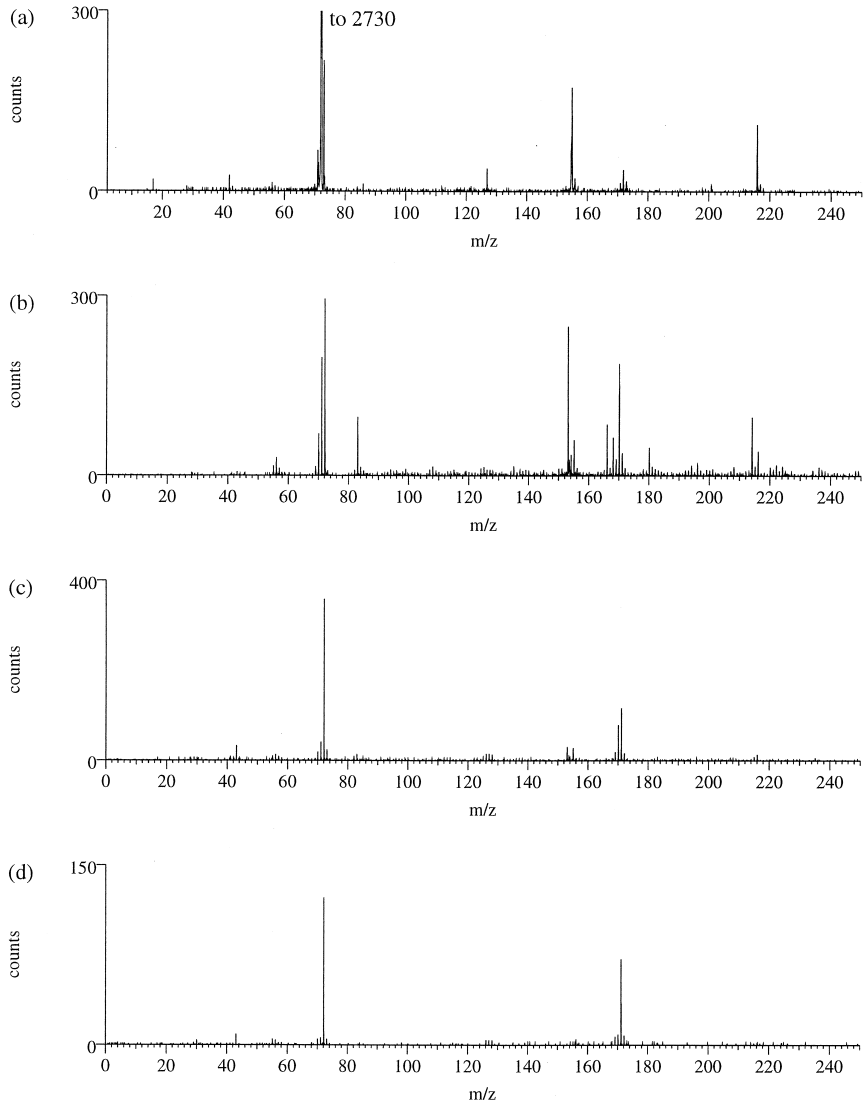

Fig. 3. Fs-MPI and SPI mass spectra of valyl-valine at threshold power density: (a) 118 nm, 20 W cm^{-2}; (b) 266 nm, 2×10^{10} W cm^{-2}; (c) 400 nm, 2×10^{11} W cm^{-2}; (d) 800 nm, 2×10^{12} W cm^{-2}.

Table 1
Normalised intensity values for valyl-valine fragment ions at threshold laser intensity

	M	M-HCOOH	M-NH_2COOH	M-NH_3HCOOH	Val-COOH	Val-NH_2COOH
118 nm	4.0		6.2		100	0.5
266 nm	13.9	63.1	20.0	84.1	100	10.2
400 nm	3.6	21.9	7.5	8.3	100	3.6
800 nm	1.6	6.6			100	3.3

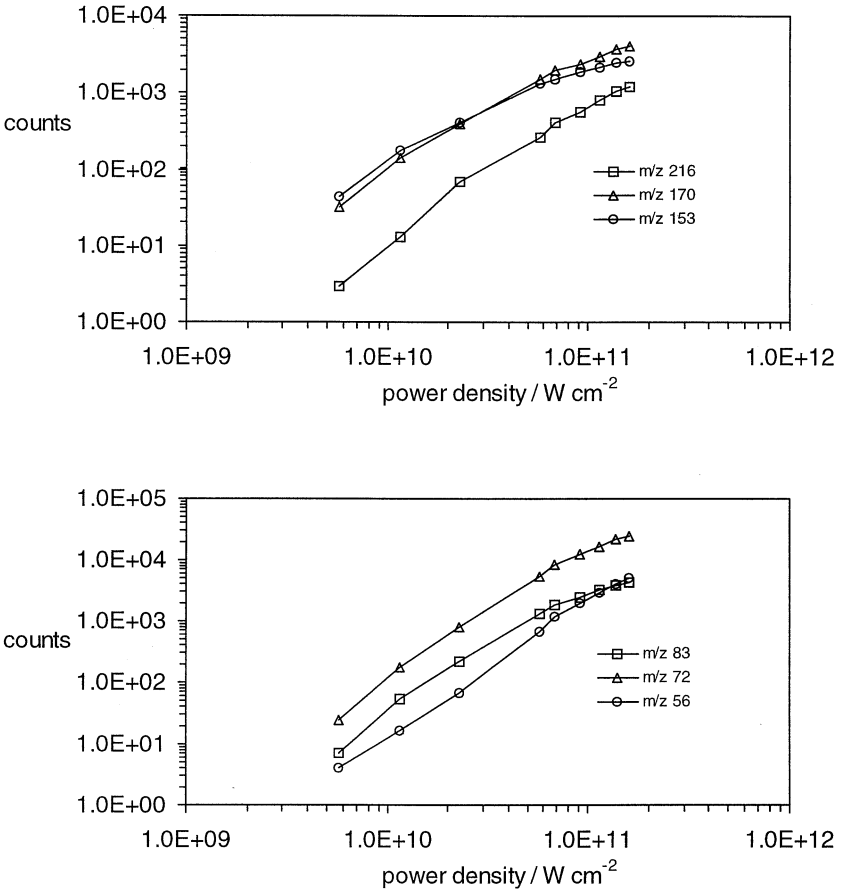

Fig. 4. 266 nm fs-MPI power plots for valyl-valine fragment ions.

higher order photon processes as the laser intensity increases. A shift in ion abundance toward lower mass is typically observed in MPI mass spectra as the laser intensity is increased and the probability of higher-order photon absorption increases [38]. The *m/z* 56 ion would appear to have at least one three-photon formation mechanism, resulting in an observed gradient >2.0. This may also be true for *m/z* 72 (val-COOH) and *m/z* 83 [$(CH_3)_2CCHCO$]. The *m/z* 56 ion continues to display the same photon order over the entire intensity range, either because it does not further fragment or because loss to a fragmentation channel is offset by a new formation mechanism operating at a comparable rate. The measured power

Table 2
Experimentally observed fs-MPI photon orders for ion signals from valyl-valine at 266, 400, and 800 nm. Linear least-squares lines have been fitted over the linear section of the relevant graphs

m/z	216	170	153	83	72	56
Species	M	M-HCOOH	M-HCOOH-NH_3	$(CH_3)_2CCHCO$	Val-COOH	Val-NH_2COOH
266 nm	1.8 ± 0.2	1.5 ± 0.1	1.2 ± 0.1	2.0 ± 0.1	2.1 ± 0.1	2.3 ± 0.1
400 nm	2.3 ± 0.1	2.0 ± 0.1	2.0 ± 0.1	2.7 ± 0.1	2.5 ± 0.1	3.1 ± 0.1
800 nm	3.8 ± 0.1	3.9 ± 0.1	3.4 ± 0.1	3.3 ± 0.1	3.5 ± 0.2	5.3 ± 0.2

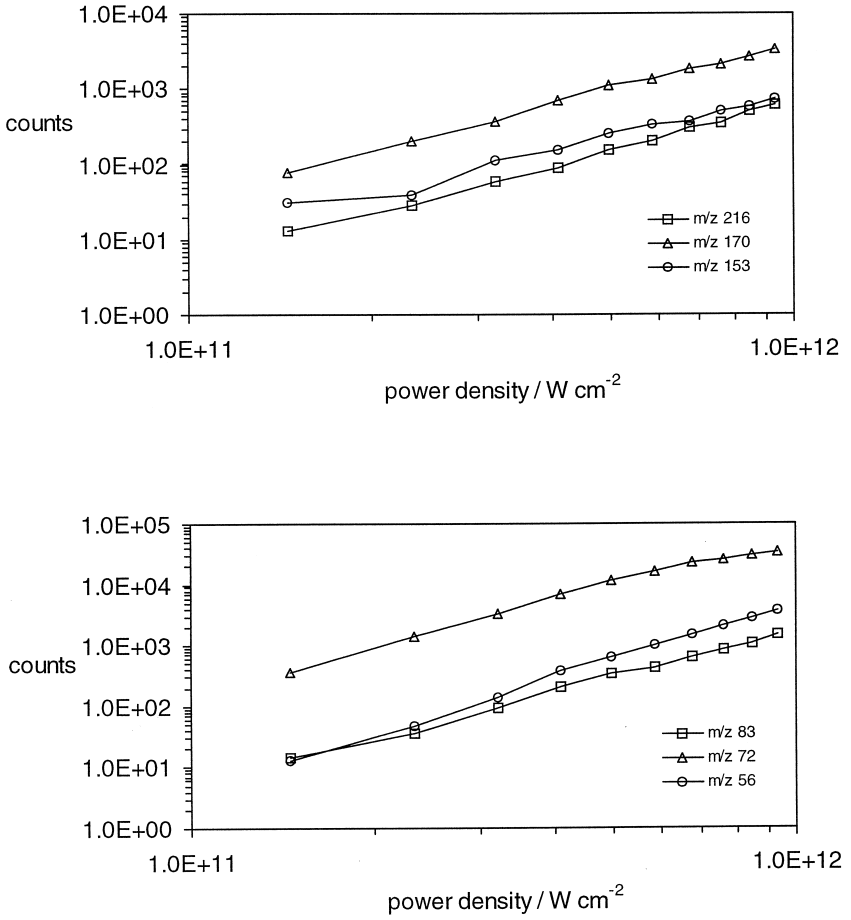

Fig. 5. 400 nm fs-MPI power plots for valyl-valine fragment ions.

dependence for the fragment ions *m/z* 170 (M-HCOOH) and *m/z* 153 (M-NH_3HCOOH) are significantly lower (1.2 and 1.5, respectively) than that expected for a two-photon process. This may be due to the efficient photofragmentation of these species as the power density is increased—the plots for these species show the greatest deviation from linearity at high power. Alternatively, a one-photon ionisation mechanism may exist for these species if they are formed as highly excited neutrals during the thermal desorption.

Fig. 5 shows the fragment ion power plots for valyl-valine at 400 nm. The plots are consistent with a three-photon formation mechanism with the possible exception of *m/z* 56 that may in part be formed by the absorption of at least one additional photon. Only the *m/z* 72 ion clearly displays a change in gradient as the intensity increases, suggesting that this species is most prone to further photofragmentation by higher-order processes.

The fragment ion power plots for valyl-valine at 800 nm are shown in Fig. 6. The gradients for the individual fragments are given in Table 2. The highest order power dependence observed is 5.3 for *m/z* 56 and also for the ions C^+ and H^+ (not shown). The higher-mass fragments and the molecular ion display a photon order that is significantly less than that expected for this wavelength. A possible reason for this is discussed in the following section.

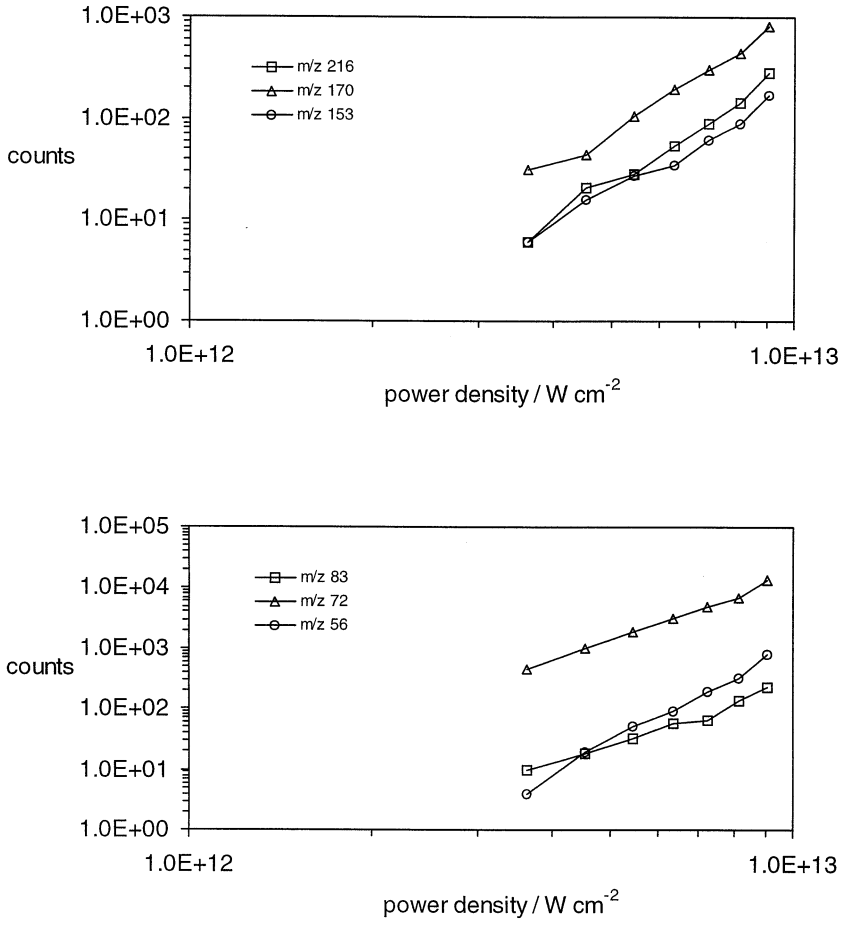

Fig. 6. 800 nm fs-MPI power plots for valyl-valine fragment ions.

3.3. Photoionisation mechanism

The laser intensity dependence of the total ion signal provides an indication of the dominant ionisation mechanism [39]. A simple multiphoton excitation mechanism yields a straight line in a log–log plot with a gradient equal to the photon order of the rate-determining step for ionisation. Note that the valyl-valine molecule does not contain a chromophoric group at any of the applied wavelengths and therefore the photon absorption is nonresonant in nature.

Fig. 7 shows the variation in the estimated useful yield as a function of laser wavelength, power density, and focal volume (in mm^3). The laser power density is attenuated as described above and the focal volume in the ionisation region is controlled by translating the focusing lens along the laser beam axis. The numbers against each data set in the figure correspond to the estimated ionisation volume in mm^3. The useful yield is the ratio of the total measured ion count to the estimated number of neutral molecules in the ionisation volume. Within the parameter of useful yield are contributions from the transmission of the spectrometer and efficiency of the detection system. In collecting this data the neutral density and the detector gain were kept constant so yields from different wavelengths could be compared. The local pressure of analyte in the ionisation volume is assumed to be 5×10^{-7} mb, an order of magnitude greater than the measured static pressure within the analysis chamber.

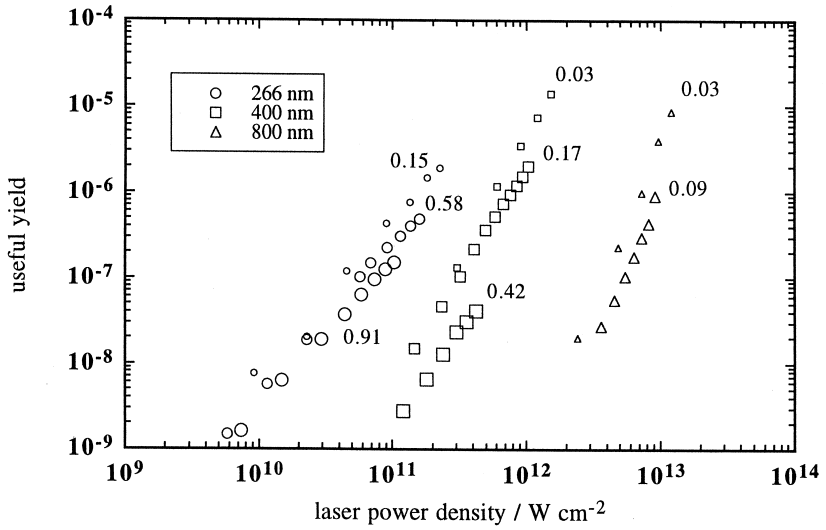

Fig. 7. Variation in estimated useful yield of photoions with wavelength, intensity, and ionisation volume (given in mm^2 next to each plot).

The ionisation volume is taken to be a cylinder of 1 mm length and diameter equal to that of the laser in the extraction axis of the spectrometer. This does not take into account the fact that the effective ionisation volume depends on the photon order and absorption cross section, but in the absence of this information provides a useful approximation. The gradients of the plots increase as the photon energy decreases, in agreement with the general prediction of perturbation theory. Linear least-squares fits have been performed on the data in Fig. 7 and the results are given in Table 3.

The ionisation potential of valyl-valine is not known but is expected to be in the range 8.0–9.0 eV given that that of valine is 8.7 eV [40]. The absorption of two photons at 266 nm (4.66 eV) is therefore expected to be sufficient to bring about ionisation of the valyl-valine molecule. The total ion signal displays a gradient of about 1.8 that is consistent with a two-photon nonresonant ionisation. A slight decrease in gradient is observed at laser intensities in the region of 10^{11} W cm^{-2} implying the possible onset of saturation effects. Saturation can occur by approaching ionisation saturation and significantly depleting the neutral population or by overloading the detector system. Because the estimated useful yields vary over a similar range for each wavelength and only the 266 nm data indicates the onset of saturation, this cannot be attributed to saturation of the ionisation. The TDC is capable of recording only one ion arrival event per 10 ns time channel per laser shot and a maximum of 256 events per shot. At 10^{11} W cm^{-2} the number of counts per time channel in the base peak of the 266 nm spectra is of the same order of magnitude as the number of laser shots so saturation of the counting is to be expected. Analogue counting electronics would prevent this problem.

At 400 nm the gradient of the total photoion

Table 3
Effect of ionisation wavelength and volume on experimentally determined power dependence of total ion yield from valyl-valine

Laser waist area/mm^2	0.91	0.58	0.15	0.42	0.17	0.03	0.09	0.03
266 nm	1.72	1.75	1.82					
400 nm				2.21	2.52	2.88		
800 nm							3.68	3.80

current is about 2.5, which is reasonably consistent with a three-photon ionisation mechanism. No saturation effects are evident and the data plot remains linear over the entire intensity range.

With 800 nm photons (1.55 eV) a six-photon ionisation mechanism is expected for this molecule. The power plot for the total ion signal displays a gradient of only about 3.7. The plot remains linear over the applied intensity range implying that saturation is not occurring. There are two possible explanations for the lower than expected power dependence. First, an excited electronic state could be populated by a four-photon nonresonant absorption. This process would constitute a rate-determining step for ionisation, with the absorption of a further two photons to reach the ionisation potential (IP) being saturated over the entire power range. Alternatively, a field ionisation mechanism could be operating to some extent. In the power density range of our 800 nm experiment (2×10^{12}–1×10^{13} W cm^{-2}) an evaluation of the Keldysh parameter finds $2.7 < \gamma < 6.0$ for species with IP = 8.5 eV and the threshold for barrier suppression is 2.1×10^{13} W cm^{-2}. Therefore we are in the intensity range where a competition between pure multiphoton and field ionisation regimes is to be expected assuming atomlike behaviour. On this basis we infer that the observed power dependency for 800 nm ionisation is most likely inadequately described by LOPT because of a transition toward a field ionisation mechanism—probably tunneling.

3.4. Relative ionisation efficiency

For each fs-MPI wavelength, as the ionisation volume decreases the useful yield increases as the efficiency of the extraction into the spectrometer increases (Fig. 7). As the laser intensity (I) increases the effective ionisation volume will expand at the rate of $I^{3/2}$ according to Gaussian beam theory [41]. This may explain why the slopes are less than integer. As the focusing becomes looser and the ionisation volume increases, the gradients become smaller. We attribute this to the intensity-induced expansion of the beam into areas in which the extraction efficiency is lower, and therefore the rate of increase in useful yield with intensity is less.

Comparable useful yields of photoions result from femtosecond excitation at 266, 400, and 800 nm over the available laser intensities at each wavelength. It should be noted that by using nanosecond laser pulses of 266 nm we have been unable to generate significant ion signals from valyl-valine at any power up to 10^9 W cm^{-2} [42].

A comparison of photofragmentation at constant useful yield is given in Fig. 8. Under these conditions ionisation with 400 and 800 nm photons results in similar degrees of fragmentation, with 266 nm ionisation resulting in slightly less. The normalised intensity values of diagnostic analyte ions under conditions of comparable useful yield are given in Table 4. The excess energy deposited in the molecular ion by the photon absorption that takes it over the ionisation potential is equivalent at each of the Ti:sapphire wavelengths used assuming an IP of 8–9 eV. This suggests that additional photon absorption is responsible for the greater fragmentation at longer wavelength and higher photon fluxes. At above-threshold laser intensity it becomes increasingly likely that more than the minimum required number of photons will be absorbed by the neutral and increasing amounts of excess energy will be available to the photoion, resulting in photofragmentation. This is illustrated by the significant abundance of nonspecific low-mass hydrocarbon fragments in Fig. 8(b)–(d).

SPI with 100 nJ cm^{-2} pulses at 118 nm (20 W cm^{-2}) gives useful yields comparable to 25 mJ cm^{-2} at 266 nm (10^{11} W cm^{-2}), 230 mJ cm^{-2} at 400 nm (10^{12} W cm^{-2}), and 1.3 J cm^{-2} at 800 nm (10^{13} W cm^{-2}). At these power densities fs-MPI results in substantially *more* fragmentation than SPI. Because of the relatively low power density of the 118 nm beam the probability of multiphoton excitation is negligible. The absorption of two 118 nm photons would deposit 21 eV into the molecule that would be sufficient to produce C^+ ions (IP = 11.26 eV). The SPI spectrum shows no significant ion abundance below the mass of the immonium ion implying that excess VUV photon absorption is minimal.

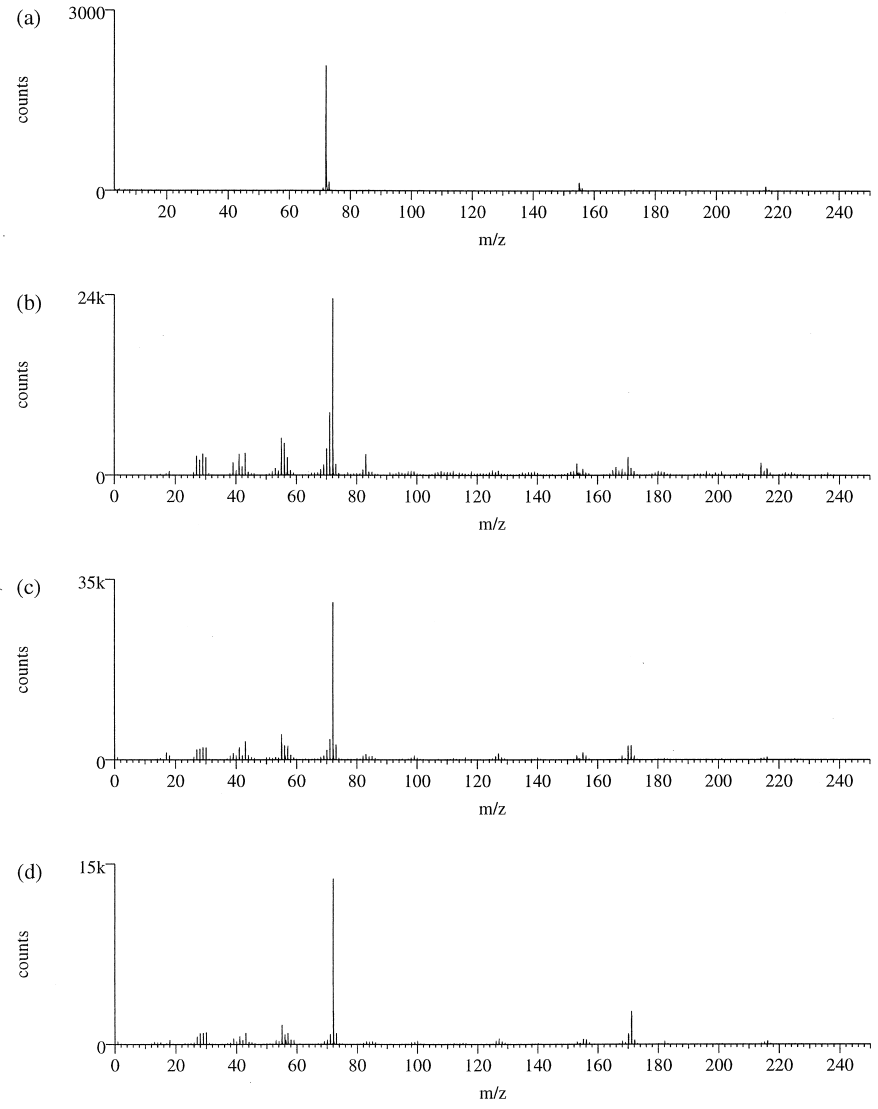

Fig. 8. Comparison of photofragmentation at constant useful yield using (a) 118 nm, (b) 266 nm, (c) 400 nm, and (d) 800 nm.

Table 4
Normalised intensity values for valyl-valine fragment ions using SPI and fs-MPI at constant useful yield

	M	M-HCOOH	M-NH_2COOH	M-NH_3HCOOH	Val-COOH	Val-NH_2COOH
118 nm	3.3		6.2		100	
266 nm	3.5	10.3	3.4	6.4	100	18.4
400 nm	1.6	8.5	4.5	2.0	100	9.2
800 nm	2.0	6.0	3.1	1.2	100	5.7

4. Conclusions

On the basis of experiments on valyl-valine, SPI using a nanosecond Nd:YAG laser compares favourably with fs-MPI in terms of minimising fragmentation without sacrificing useful yield. The ionisation efficiency of nonresonant fs-MPI is only able to match that of SPI at high laser intensity conditions that lead to increased fragmentation and reduced molecular information compared to SPI.

There are features of both approaches that make them very useful analytical tools. Femtosecond MPI has the advantage in that variable degrees of photofragmentation can be induced, which may provide additional information on molecular structure and insights into the photoionisation–dissociation mechanism. The SPI spectra are very reproducible and inherently insensitive to fluctuations in laser power density. In this sense SPI data is ideally suited for spectral fingerprinting.

From the laser intensity dependence of the total ion signal we conclude that fs-MPI using 266 or 400 nm photons is adequately described by LOPT. For 800 nm (2×10^{12}–1×10^{13} W cm^{-2}) photonionisation, however, we infer that both multiphoton and field ionisation mechanisms are operative.

In summary, both SPI and fs-MPI are effective methods for producing radical molecular ions and diagnostic fragments from the fragile molecule valyl-valine despite the absence of a chromophore for multiphoton excitation. As such, both methods show promise for the detection of a wide variety of biomolecular types.

Acknowledgements

The authors would like to thank Prof. Nick Winograd of Penn State University for use of the Ti:sapphire laser. The financial support of EPSRC is gratefully acknowledged (GR/K44015, GR/L58606).

References

[1] J. Grotemeyer, K. Walter, U. Boesl, E.W. Schlag, Int. J. Mass Spectrom. Ion Processes 78 (1987) 69.
[2] R. Trembreull, D.M. Lubman, Anal. Chem. 59 (1987) 1003.
[3] J. Grotemeyer, E.W. Schlag, Angew. Chem. Int. Ed. Engl. 27 (1988) 447.
[4] D.M. Hrubowchak, M.H. Ervin, M.C. Wood, N. Winograd, Anal. Chem. 63 (1991) 225.
[5] M. Terhorst, G. Kampwerth, E. Niehuis, A. Benninghoven, J. Vac. Sci. Technol. A10 (1992) 3210.
[6] M.H. Ervin, M.C. Wood, N. Winograd, Anal. Chem. 65 (1993) 417.
[7] R. Trembreull, D.M. Lubman, Anal. Chem. 59 (1987) 1003.
[8] C. Grun, R. Heinicke, C. Weickhardt, J. Grotemeyer, Int. J. Mass Spectrom. 185 (1999) 307.
[9] R. Möllers, M. Terhorst, E. Niehuis, A. Benninghoven, Org. Mass Spectrom. 27 (1992) 1393.
[10] C.L. Brummel, K.F. Willey, J.C. Vickerman, N. Winograd, Int. J. Mass Spectrom. Ion Processes 143 (1995) 257.
[11] K.F. Willey, V. Vorsa, R.M. Braun, N. Winograd, Rapid Commun. Mass Spectrom. 12 (1998) 1253.
[12] R. Weinkauf, P. Aicher, G. Wesley, J. Grotemeyer, E.W. Schlag, J. Phys. Chem. 98 (1994) 8381.
[13] S. Wei, J. Puernell, S.A. Buzza, R.J. Stanley, A.W. Castleman Jr., J. Chem. Phys. 97 (1992) 9480.
[14] K.W.D. Ledingham, H.S. Kilic, C. Kosmidis, R.M. Deas, A. Marshall, T. McCanny, R.P. Singhal, A.J. Langley, W. Shaikh, Rapid Commun. Mass Spectrom. 9 (1995) 1522.
[15] M.J. DeWitt, R.J. Levis, J. Chem. Phys. 102 (1995) 8670.
[16] M.J. DeWitt, D.W. Peters, R.J. Levis, Chem. Phys. 218 (1997) 211.
[17] K.W.D. Ledingham, R.P. Singhal, Int. J. Mass Spectrom. Ion Processes 163 (1997) 149.
[18] U. Schuhle, J.B. Pallix, C.H. Becker, J. Am. Chem. Soc. 110 (1988) 2323.
[19] S.E. Van Bramer, M.V. Johnston, J. Am. Soc. Mass Spectrom. 1 (1990) 419.
[20] C. Köster, J. Grotemeyer, Org. Mass Spectrom. 27 (1992) 463.
[21] C.R. Ayre, L. Moro, C.H. Becker, Anal. Chem. 66 (1994) 1610.
[22] J.L. Trevor, K.R. Lykke, M.J. Pellin, L. Hanley, Langmuir 14 (1998) 1664.
[23] V.S. Letokhov, Laser Photoionisation Spectroscopy, Academic, New York, 1987.
[24] L.V. Keldysh, Sov. Phys. JETP 20 (1965) 1307.
[25] S. Augst, D.D. Meyerhofer, D. Strickland, S.L. Chin, J. Opt. Soc. Am. B 8 (1991) 858.
[26] F.A. Ilkov, J.E. Decker, S.L. Chin, J. Phys. B: At. Mol. Opt. Phys. 25 (1992) 4005.
[27] S. Augst, D. Strickland, D.D. Meyerhofer, S.L. Chin, J.H. Eberly, Phys. Rev. Lett. 63 (1989) 2212.
[28] T.D.G. Walsh, F.A. Ilkov, J.E. Decker, S.L. Chin, J. Phys. B: At. Mol. Opt. Phys. 27 (1994) 3767.
[29] M.J. DeWitt, R.J. Levis, J. Chem. Phys. 102 (1995) 8670.
[30] A. Conjusteau, A.D. Bandrauk, P.B. Corkum, J. Chem. Phys. 106 (1997) 9095.
[31] K.F. Willey, C.L. Brummel, N. Winograd, Chem. Phys. Lett. 267 (1997) 359.
[32] M.J. DeWitt, R.J. Levis, J. Chem. Phys. 108 (1998) 7045.
[33] A.H. Kung, J.F. Young, S.E. Harris, Appl. Phys. Lett. 22 (1976) 301.

[34] A.H. Kung, J.F. Young, S.E. Harris, Appl. Phys. Lett. 28 (1976) 294.
[35] N.P. Lockyer, J.C. Vickerman, Laser Chem. 17 (1997) 139.
[36] M. Dey, J. Grotemeyer, Org. Mass Spectrom. 29 (1994) 659.
[37] B.D. Koplitz, J.K. McVey, J. Chem. Phys. 80 (1984) 2271.
[38] R.B. Bernstein, J. Phys. Chem. 86 (1982) 1178.
[39] W. Dietz, H.J. Neusser, U. Boesl, E.W. Schlag, S.H. Lin, Chem. Phys. 66 (1982) 105.
[40] S. Campbell, J.L. Beauchamp, M. Rempe, D.L. Lichtenberger, Int. J. Mass Spectrom. Ion Processes 117 (1992) 83.
[41] D.E. Mattern, Anal. Chem. 56 (1984) 2762.
[42] N.P. Lockyer, J.C. Vickerman, Int. J. Mass Spectrom. Ion Processes 176 (1998) 77.